Tellus
SERIES A
DYNAMIC
METEOROLOGY
AND OCEANOGRAPHY
PUBLISHED BY THE INTERNATIONAL METEOROLOGICAL INSTITUTE IN STOCKHOLM

Tellus (2010), 62A, 202–208

TELLUS

Climatology and variability of Southern Hemisphere marine cold-air outbreaks

By THOMAS J. BRACEGIRDLE[1]* and ERIK W. KOLSTAD[2], [1]*British Antarctic Survey, Cambridge CB3 0ET, United Kingdom;* [2]*Bjerknes Centre for Climate Research, Bergen, Norway*

(Manuscript received 18 August 2009; in final form 3 December 2009)

ABSTRACT

Marine cold air outbreaks (MCAOs) are events where cold air flows over a relatively warm sea surface. Such outbreaks are associated with severe mesoscale weather systems that are not generally resolved in global climate models, such as polar lows and boundary-layer fronts. Here, an analysis of winter climatology and variability of MCAOs in the Southern Hemisphere (SH) is presented. Near the sea ice edge, north–south fluctuations of the Southern Annular Mode (SAM) index are key, while further north, large-scale wave disturbances are needed to move air masses far enough away from the Antarctic continent to instigate MCAOs. Unlike in the Northern Hemisphere (NH), the spatial patterns of mean and extreme values of the MCAO index differ considerably. Near 60°S, both mean and extreme values of the index are similar to those found in the main MCAO regions in the NH. Further north, the mean MCAO index is quite high, but the extreme values are much lower than in the NH. We conclude that MCAOs in the SH are as widespread and can be as strong as in the NH, but severe MCAOs near densely populated regions such as the Tasman Sea are less common than in the Nordic Seas and near Japan.

1. Introduction

Marine cold air outbreaks (MCAOs) are characterized by the advection of a cold air mass over a relatively warm sea surface. They are associated with severe mesoscale weather phenomena, most notably boundary-layer fronts and polar lows (Carleton and Song, 1997; Grønås and Skeie, 1999; Rasmussen and Turner, 2003). MCAOs have been characterized and studied to some extent in all parts of the NH (Grønås and Kvamstø, 1995; Dorman et al., 2004; Kolstad and Bracegirdle, 2008; Kolstad et al., 2009). To date, however, they have not been systematically assessed in the Southern Hemisphere (SH). In this study, we assess the climatological severity and seasonal variability of MCAOs across the SH, as well as the association between large-scale atmospheric circulation variability and MCAOs.

The potential for intense boundary-layer fronts and polar lows is increased during severe MCAOs. Boundary-layer fronts, sometimes referred to as arctic fronts, are the leading edges of MCAOs and are quite common in the Nordic Seas region close to the sea ice edge in winter. Large heat fluxes over the ocean in the vicinity of boundary-layer fronts can enhance frontogenesis, which, in many cases, will cause strengthening of a potentially damaging near-surface jet (Økland, 1998; Grønås and Skeie, 1999). Polar lows are an intense subset of polar mesocyclones (cyclones less than approximately 1000 km in diameter) often associated with MCAOs (Grønås and Kvamstø, 1995; Carleton and Song, 1997; Blechschmidt et al., 2009). Increased temperature differences between the sea surface and the air have been found to increase the intensity of numerically simulated polar lows (Blier, 1996; Craig and Gray, 1996). It is thought that polar lows are less common in the SH than in the NH (Rasmussen and Turner, 2003). One of the objectives of this paper is to investigate whether there is less 'potential' for polar lows, that is, frequency and strength of MCAOs, in the SH than in the NH.

Climatological analyses of satellite imagery have shown that polar mesocyclones are widespread across high southern latitudes. However, intense polar mesocyclones (polar lows) appear to be less common than over the NH since the more convective 'spiral-shaped' cloud signatures seen in satellite imagery are generally less prevalent than more baroclinic 'comma-shaped' cloud signatures (Carleton and Carpenter, 1990). However, in winter, close to the ice edge, spiral-shaped mesocyclones are more common, implying a stronger surface-atmosphere interaction. In particular, the Ross Sea shows a winter spiral/comma occurrence ratio of approximately 0.8 (Carleton and Fitch, 1993), which is comparable to the ratio seen for polar mesocyclones over the NH (Carleton, 1985; Harold et al., 1999). At lower latitudes, mesoscale lows are less common but have been found to be an important explanation for difficulties in predicting the sea state along the west coast of New Zealand. Laing and Reid

*Corresponding author.
e-mail: tjbra@bas.ac.uk
DOI: 10.1111/j.1600-0870.2009.00431.x

(1999) found that a common feature among these lows was a 'high sea minus air temperature difference', indicating an association with MCAOs. The lows are thought to be a consequence of the relatively strong interaction between cold, stably stratified air masses and orography. They are not directly linked to the 'cold air mesocyclones' found by Carleton and Song (1997) to be widespread across the southern Tasman Sea in winter, but both phenomena are problematic for human activity at sea around New Zealand and over the Tasman Sea.

Links between MCAOs in specific regions of the northern North Atlantic and larger-scale patterns of variability have been demonstrated by Kolstad et al. (2009). In both hemispheres, the annular modes are the dominant patterns of variability (Thompson and Wallace, 2000). In the SH, the leading mode is referred to as the SH Annular Mode (SAM). The SAM is more zonally symmetric than the Northern Annular Mode (NAM) and is associated with north–south movements of the low-level, eddy-driven jet around 50–60°S (Limpasuvan and Hartmann, 2000). The second and third Empirical Orthogonal Functions (EOFs) of geopotential height anomalies in the SH are not well separated but together account for much of the meridional variability. Both show strong wave trains across the southern Pacific and have been referred to as Pacific South American patterns PSA-1 and PSA-2, respectively (Lau et al., 1994; Mo, 2000). The PSAs provide a mid-to-high latitude teleconnection to ENSO variability (Karoly, 1989; Mo, 2000).

Previous studies have pointed to large-scale influences on cold air outbreaks in the SH. For instance, Carleton and Song (1997) showed that hemispheric-scale pressure patterns were associated with cold-air mesocyclones in the Australasian sector. However, their analysis was based on data from a single season. More recently, Claud et al. (2009) showed significant relationships between large-scale indicators of mesocyclones and the SAM and ENSO. Their analysis used climatological averages rather than extremes, which are considered here. We use re-analysis data spanning 31 winters to assess long-term climatology and associations between MCAOs and large-scale atmospheric circulation patterns.

In the next section, the data and methodology are outlined. The long-term climatology, in terms of both means and extremes of MCAOs across the SH, is shown in Section 3. Results from an assessment of the links with large-scale atmospheric variability are shown in Section 4, followed by the main discussion and conclusions in Section 5.

2. Data and methods

Many mesoscale weather systems are too small in size to be represented explicitly in re-analyses and most current global climate models. However, MCAOs are larger-scale features and are usually reproduced even by coarse-resolution models. The use of an MCAO index, that is, a scalar computed from quantities that are resolved even by coarse models, can therefore help to study both past variability and sensitivity to climate changes. Here, we use a slightly modified version of the MCAO index that was used in our earlier studies (Kolstad and Bracegirdle, 2008; Kolstad et al., 2009).

Climatological studies require a consistent data set to avoid effects of spurious variability or trends. Re-analysis modelling is an effort to provide such data sets by assimilating observations into a consistent modelling system. However, changes in the observing network can have an impact on accuracy. Because of the introduction of widespread satellite-retrieved atmospheric and surface data, there is a jump in accuracy in re-analysis data sets in 1979, which is particularly prominent over high southern latitudes due to the earlier dependency on sparsely distributed in situ observation stations (Bromwich et al., 2007). For high southern latitudes in the winter season, Bromwich and Fogt (2004) found the European Centre for Medium Range Weather Forecasting (ECMWF) ERA-40 re-analysis to be more reliable than the National Centers for Environmental Prediction/National Center for Atmospheric Research (NNR) re-analysis (Kalnay et al., 1996). However, a disadvantage of ERA-40 is that it terminated in 2002, whereas the NNR re-analysis is updated in real time, giving an additional seven winters of data at the time of writing. Here, we used both analyses and found that our conclusions are robust in both data sets. Only the results from NNR are shown. The analysis period is June–September (JJAS) from 1979 to 2009.

A number of parameters are considered for the analysis in this paper: the potential skin temperature, defined as $\theta_{\mathrm{SKT}} = T_{\mathrm{SK}}(p_0/p_{\mathrm{sl}})^{R/c_p}$, where T_{SK} is the skin temperature [sea surface temperature (SST) over open ocean], p_0 is 1000 hPa and p_{sl} is the sea level pressure (SLP); θ_{700}, the potential temperature at 700 hPa; and a dimensionless MCAO index, defined as $M \equiv \frac{L}{Z_{700}}(\ln\ \theta_{SKT}\ - \ln\ \theta_{700})$, where L is a scaling height of 7.5×10^5 m and Z_{700} is the geopotential height at 700 hPa. L is chosen so that under normal conditions, M is roughly the same as the vertical temperature difference $T_{\mathrm{SK}} - \theta_{700}$. For instance, if $T_{\mathrm{SK}} - \theta_{700} = 2\,^{\circ}\mathrm{C}$, the SST is 4 °C, the SLP is 1000 hPa and Z_{700} is 2700 m, then $M = 2$. The new index M is more straightforward to interpret than the MCAO index in our previous studies, as it is closely aligned to actual sea–air differences in potential temperature.

The principal component (or EOF) analysis (Jolliffe, 2002) below was performed on seasonal (JJAS) mean NNR data from 1979 to 2009. Every grid point south of 20°S was used to compute the leading principal components (PCs) of 500-hPa geopotential height anomalies.

3. Climatology

Figure 1 shows the average departure from the zonal mean skin temperature (a) and 700-hPa temperature (b) in the extra-tropical SH winter (JJAS). As the MCAO index M is roughly proportional to the vertical difference between these two parameters, Fig. 1

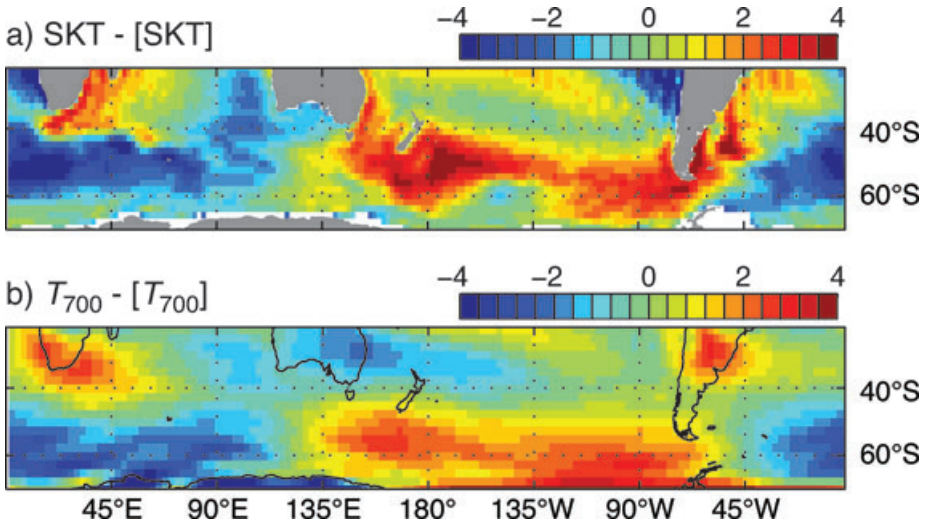

Fig. 1. Winter (JJAS) climatological departures from the zonal mean of skin temperature (a) and 700-hPa temperature (b). Note that values beyond the edges of the colour scales are not shown. In (a), only wet grid cells were included in the calculation of the zonal mean, and grid points that had sea ice more than 20% of the time were excluded.

provides a useful reference when regional differences in the spatial distribution of M are considered below.

In Fig. 2a, the mean MCAO index M_{mean} in winter is shown. The largest values (>-4) are found in a belt near the Antarctic sea ice edge from the eastern Weddell Sea at approximately 30°W to the Kerguelen Plateau at approximately 90°E. This is a region where air temperatures are quite low with respect to latitude (Fig. 1b). Large values of M_{mean} are also found east of Australia, just north of 40°S, and especially over the East Australian Current in the Tasman Sea, where SSTs are high (Fig. 1a) and air temperatures are low (Fig. 1b). In these regions, M_{mean} shows similar values to those seen over the Nordic Seas and near Japan, the regions with the highest M_{mean} values in the NH (Fig. 3a). Moderately large values (between -7 and -4) are found in a large swath of the Pacific east of New Zealand (due to low air temperatures; Fig 1b), in a stretch from the Bellingshausen Plain through the Drake Passage to the southwestern Atlantic (due to high SSTs; Fig. 1a), in a belt between southwestern Australia and the southern tip of Africa and near the Antarctic sea ice in general. In the NH, there are few regions with comparably large values: the Barents/Norwegian Sea, the Irminger and Labrador Seas, a small zone off the east coast of North America, and over large parts of the North Pacific east and northeast of Japan (Fig. 3a). The lowest M_{mean} values are found in the subtropics, in the transition zone between the South Pacific and the Southern Ocean (due to high air temperatures; Fig. 1b), as well as in a broad belt stretching eastward from the Antarctic Peninsula to the southern tip of New Zealand (due to low SSTs; Fig. 1a).

The climatological strength of MCAOs is quantified here as the 90th percentiles of the MCAO index (M_{90}), shown in Fig. 2b. By this measure, the most severe MCAOs ($M_{90} > 2$) are only found in the marginal ice zone near the Antarctic continent and in a small region of the southwestern Atlantic. It is only in these

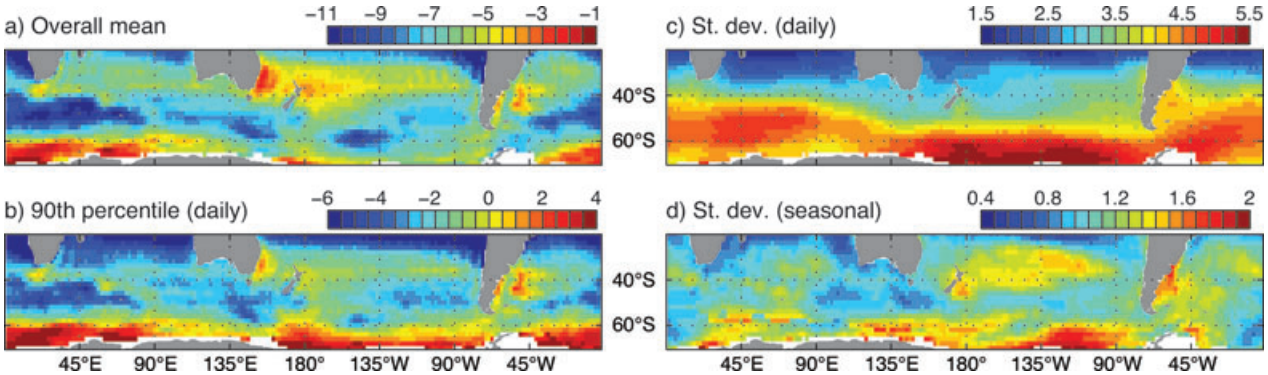

Fig. 2. Winter climatological statistics of the MCAO index: overall mean (a), 90th percentile on the daily time scale (b), standard deviation on the daily (c) and seasonal (d) time scales. Note that values beyond the edges of the colour scales are not shown. Grid points that had sea ice more than 20% of the time were excluded.

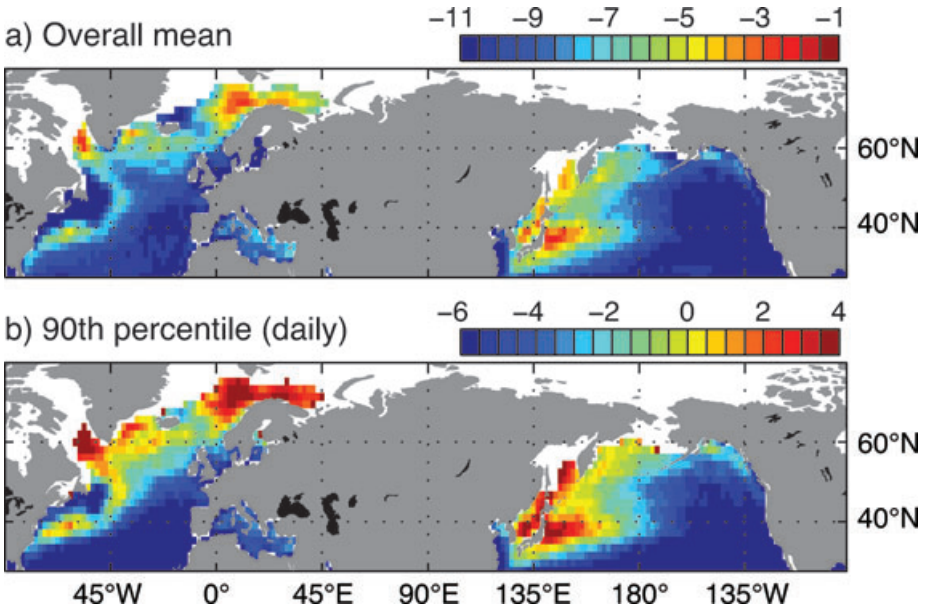

Fig. 3. As Figs. 2a–b, but for the NH winter (DJFM).

regions that M_{90} is as large as in the primary MCAO regions in the NH, the Barents, Norwegian and Labrador Seas and the areas both east and west of Japan (Fig. 3b).

In Figs. 2c and d, the standard deviation of M on daily (c) and seasonal (d) time scales are shown. The spatial distribution of the variance of M can be partly understood by examining the extra-tropical storm track. In a broad band around 60°S, the variance is large, but at lower latitudes, such as over the Tasman Sea, the variance is quite low. The main region of large daily variance, in addition to the marginal ice zones, is collocated with the SH extra-tropical storm track, which spirals inward from a major genesis region over southern South America towards the Antarctic coast line (Inatsu and Hoskins, 2004; Hoskins and Hodges, 2005).

The daily variability is dominated by the air temperature (not shown), as is seen over the NH (Kolstad et al., 2009). On monthly and seasonal time scales, the picture is more complex. Although not shown here, the variance pattern in Fig. 2c is almost identical to the variance pattern of the 700-hPa temperature, while the variance on the seasonal time scale (Fig. 2d) is influenced by SST variations as well. We now use linear regression to assess the relative importance of SSTs and air temperatures with respect to M on these time scales. Two regression models were used: (1) a multivariate model with skin and air temperatures as regressors, which explains nearly all of the variance and (2) a univariate model with air temperature as the sole regressor.

In Fig. 4a, the ratio of the regression coefficient of skin temperature to the coefficient of negative 700-hPa air temperatures

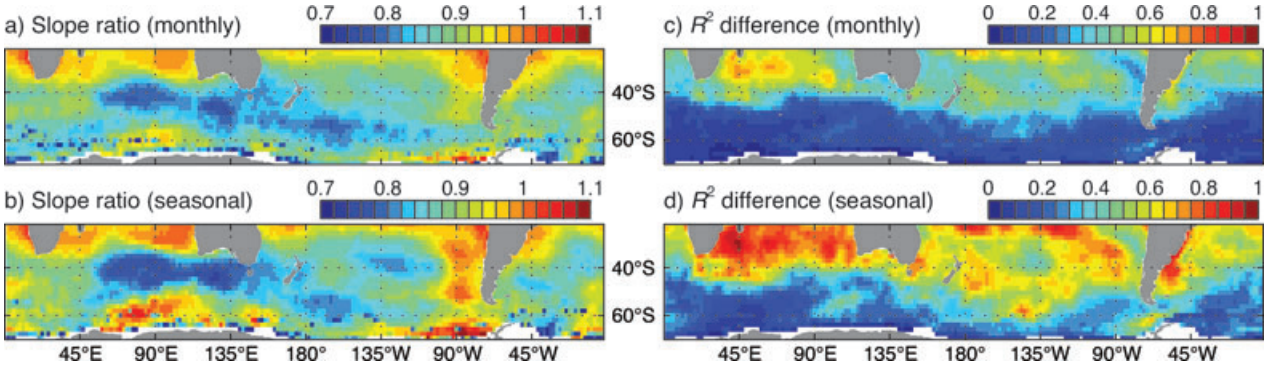

Fig. 4. Linear regression with the MCAO index as the regressand. (a, b) The regression coefficient of skin temperature divided by the coefficient of 700-hPa air temperature. (c, d) The R^2-value of the bivariate regression model minus the R^2-value of a univariate regression model with 700-hPa temperature as the sole regressor. Monthly (upper panels) and seasonal (lower panels) means were used, and grid points that had sea ice more than 20% of the time were excluded.

in the multivariate model and on the monthly time scale is shown for each grid point. The same ratio on the seasonal time scale is shown in Fig. 4b. Grid points that had sea ice more than 20% of the time were excluded and are shown in white. Note that there is some noise near the sea ice edge. A 1° change in air temperature has an equal or larger influence on the magnitude of M than a similar change of SST in large parts of the SH (as illustrated by low values of the ratio). In a band to the south of Australia and New Zealand, the influence of air temperature is especially large. This is logical because this band coincides with a region of relatively low climatological M mean values and variance (Fig. 2). Thus, a one-degree change in air temperature produces a larger change in M in this band than in a region with a higher mean values and variance. Moreover, this band is approximately collocated with a region of low cyclonic density in the winter SH storm track (Hoskins and Hodges, 2005). Outside the marginal ice zone and the subtropics, the largest ratio values (indicating the largest relative influence of SSTs on M) are found off the west coast of South America.

In Figs. 4c and d, the difference between the R^2-value of the multivariate model and the univariate model with air temperature as the sole regressor is shown on monthly and seasonal time scales, respectively. In other words, Figs. 4c and d show how much added variance the regression model explains if SSTs are included, compared to a model that only includes air temperatures. In the extra-tropical storm track, poleward of approximately 45°, air temperature fluctuations account for virtually all of the variance on the monthly time scale (Fig. 4c). In the subtropics, there are regions where SSTs are needed to explain the variance, particularly in the Indian Ocean and large parts of the South Pacific, on a seasonal time scale.

4. Links with large-scale patterns of variability

It was found that there is a strong correlation between the inter-annual variability of winter M_{mean} and M_{90}. The zonal mean of pointwise correlations at 60°S is 0.75, which is similar to values over key regions over the northern North Atlantic (Kolstad et al., 2009). This shows that the strength of MCAOs (M_{90}) in a given season is strongly related to large-scale seasonal anomalies in the atmosphere and/or ocean. In the previous section, a strong link between the variability of M and the SH storm track was suggested. This motivates an assessment of links with the SAM, which is associated with vacillations of the extra-tropical storm tracks across the latitude band from approximately 40°S to 60°S (Limpasuvan and Hartmann, 2000).

Using seasonal means of 500-hPa geopotential height, EOFs were computed for the SH poleward of 20°S. The cumulative explained variance of the first five EOFs was 31, 47, 61, 67 and 72%, respectively. As mentioned earlier, the second and third EOFs are not well separated. We now use the first three PCs as regressors in a multiple regression model with seasonal means of M as the regressand. The loading patterns of the PCs are expressed as their regression coefficients in Figs. 5a–c. The explained variance of: (1) a univariate model with PC 1 as the sole regressor is shown in Fig. 5d, (2) a multivariate model with PCs 2 and 3 as regressors is shown in Fig. 5e and (3) the full multivariate model is shown in Fig. 5f.

There is a strong, positive relationship between the seasonal time series of the SAM (PC 1) and wintertime M_{mean} over ice-free regions off most of the Antarctic coastline (Figs. 5a and d). This is consistent with the well-documented atmospheric temperature response to the SAM, which generally shows cold

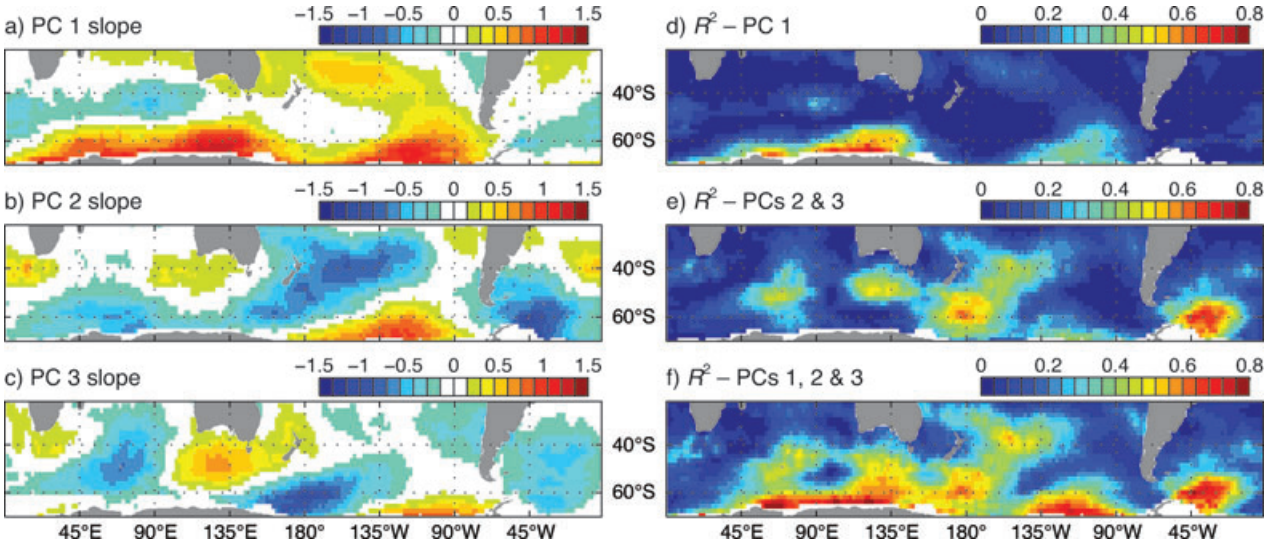

Fig. 5. Results from regression models with three leading PCs as regressors and M as the regressand. (a–c) The regression coefficients of the first three PCs in a multivariate model. The unit is M units per standard deviation unit. (d) The R^2-value of a univariate model with PC 1 as the sole regressor. (e) The R^2-value of a multivariate model with PCs 2 and 3 as regressors. (f) The R^2-value of a multivariate model with PCs 1–3 as regressors.

(warm) tropospheric temperature anomalies over and around Antarctica in response to a positive (negative) polarity of the SAM (Gillett and Thompson, 2003; Marshall, 2007). Further north, at mid-to-low latitudes, the SAM is no longer strongly related to M_{mean}. Here, PCs 2 and 3 (PSA-1 and PSA-2) are more important, particularly around New Zealand and Australia and north of East Antarctica (Figs. 5b–c and e). The relationship between the PSA patterns and M_{mean} extends to the Antarctic coastline around the Peninsula region. The region to the west of the Peninsula, where the variance of M is large (Figs. 2c–d), is an example of a region where all of the three leading PCs have large regression coefficients (Fig. 5a–c) and where these three together explain a large share of the seasonal variance of M.

5. Summary and discussion

In this study, the climatology and variability of winter (June–August) MCAOs in the SH have been assessed. The study was based on data from both NCEP/NCAR and ERA-40 re-analyses. The MCAO index here is a slightly modified version of that introduced by Kolstad and Bracegirdle (2008) and Kolstad et al. (2009). The new index M is more straightforward to interpret, as it is closely aligned to actual sea–air differences in potential temperature.

The climatological average MCAO index, M_{mean}, is comparable in magnitude over primary regions in both hemispheres, but relatively high M_{mean} values cover larger regions in the SH than in the NH. However, climatological extremes of the MCAO index (the 90th percentile, M_{90}) are weaker away from the marginal ice zones in the SH than in the NH, most likely due to a smaller daily variance of M. One exception is over the open ocean adjacent to the sea ice around Antarctica, where due to a large daily variance, M_{90} is comparable in magnitude to the values over the Nordic Seas, the Labrador Sea and over the ocean near Japan. In other words, the potential for severe high-latitude weather, such as polar lows and boundary-layer fronts, is as large near the marginal ice zone in the SH as in the well-known polar low 'hotspots' in the NH.

The spatial distribution of the MCAO index is consistent with the observation that mesocyclones are generally less convective in the SH than in the NH (Rasmussen and Turner, 2003). Indeed, Carleton and Carpenter (1990) found that almost all of the convective ('spiraliform') polar lows they identified over the SH occurred near to the sea ice edge, consistent with the spatial climatology of M_{90}. Unresolved mesocyclones in these regions might be a source of significant errors in surface heat fluxes, as was found over the northern North Atlantic by Condron et al. (2008).

The strongest variability of MCAOs follows the lower-tropospheric extra-tropical storm track, which spirals inward from southern South America towards the Antarctic coast (Hoskins and Hodges, 2005). The different spatial patterns of the mean compared to extreme MCAO index show that factors controlling their intensity, such as storm tracks and SST variability, vary in importance spatially. This has implications for understanding how forced and internal climate variability may influence MCAOs. For instance, studies of trends in extreme cold-air outbreaks over land have found that in some cases, they do not follow the local mean trend due to atmospheric circulation changes, a phenomenon referred to as the climate paradox (Vavrus et al., 2006). Long-term changes were not assessed from the re-analysis data due to possible spurious trends generated by issues such as variations in the observation network (Marshall, 2002).

The inter-annual variability of winter M_{mean} was found to be related to the SAM (the first PC of 500-hPa geopotential height south of 20°S) over ice-free regions around Antarctica. Regions of positive and negative correlations with the SAM are broadly similar to the associations between the SAM and a polar mesocyclone activity index used by Claud et al. (2009). However, as the SAM mainly governs shifts of the zonal mean jet structure, it was found that PCs 2 and 3, which are less zonally symmetric, are more important for MCAOs at mid-to-high latitudes. This is particularly apparent off southern Australia, to the south and west of New Zealand, and north of East Antarctica. One should be careful not to interpret the links between MCAOs and the first three patterns of variability too literally. PCs 2 and 3 are not well separated and may be degenerate. However, an important result of our analysis is that the temporal and spatial distributions are not entirely described by the SAM, especially at lower latitudes.

6. Acknowledgments

The authors thank the reviewers for their useful and constructive comments. Erik Kolstad's work was funded by the Norwegian Research Council through its International Polar Year programme and the project IPY-THORPEX (grant number 175992/S30). This is publication no. A256 from the Bjerknes Centre for Climate Research.

References

Blechschmidt, A. M., Bakan, S. and Grassl, H. 2009. Large-scale atmospheric circulation patterns during polar low events over the Nordic seas. *J. Geophys. Res.* **114**, D06115, doi:10.1029/2008jd010865.

Blier, W. 1996. A numerical modeling investigation of a case of polar airstream cyclogenesis over the Gulf of Alaska. *Mon. Wea. Rev.* **124**, 2703–2725.

Bromwich, D. H. and Fogt, R. L. 2004. Strong trends in the skill of the ERA-40 and NCEP-NCAR reanalyses in the high and midlatitudes of the southern hemisphere, 1958–2001. *J. Clim.* **17**, 4603–4619.

Bromwich, D. H., Fogt, R. L., Hodges, K. I. and Walsh, J. E. 2007. A tropospheric assessment of the ERA-40, NCEP, and JRA-25 global reanalyses in the polar regions. *J. Geophys. Res.* **112**, D10111, doi:10.1029/2006jd007859.

Carleton, A. M. 1985. Satellite climatological aspects of the "polar low" and "instant occlusion". *Tellus* **37A**, 433–450.

Carleton, A. M. and Carpenter, D. A. 1990. Satellite climatology of 'polar lows' and broadscale climatic associations for the southern hemisphere. *Int. J. Climatol.* **10**, 219–246.

Carleton, A. M. and Fitch, M. 1993. Synoptic aspects of Antarctic mesocyclones. *J. Geophys. Res.* **98**, 12997–13018.

Carleton, A. M. and Song, Y. 1997. Synoptic climatology, and intrahemispheric associations, of cold air mesocyclones in the Australasian sector. *J. Geophys. Res.* **102**, 13873–13887.

Claud, C., Carleton, A. M., Duchiron, B. and Terray, P. 2009. Southern hemisphere winter cold-air mesocyclones: climatic environments and associations with teleconnections. *Clim. Dyn.* **33**, 383–408, doi:10.1007/s00382-008-0468-5.

Condron, A., Bigg, G. R. and Renfrew, I. A. 2008. Modeling the impact of polar mesocyclones on ocean circulation. *J. Geophys. Res.-Oceans* **113**, C10005, doi:10.1029/2007jc004599.

Craig, G. C. and Gray, S. L. 1996. CISK or WISHE as the Mechanism for Tropical Cyclone Intensification. *J. Atmos. Sci.* **53**, 3528–3540.

Dorman, C. E., Beardsley, R. C., Dashko, N. A., Friehe, C. A., Kheilf, D. and co-authors. 2004. Winter marine atmospheric conditions over the Japan Sea. *J. Geophys. Res.-Oceans* **109**, C12011, doi:10.1029/2001jc001197.

Gillett, N. P. and Thompson, D. W. J. 2003. Simulation of recent Southern Hemisphere climate change. *Science* **302**, 273–275.

Grønås, S. and Kvamstø, N. G. 1995. Numerical simulations of the synoptic conditions and development of Arctic outbreak polar lows. *Tellus* **47A**, 797–814.

Grønås, S. and Skeie, P. 1999. A case study of strong winds at an Arctic front. *Tellus* **51**, 865–879.

Harold, J. M., Bigg, G. R. and Turner, J. 1999. Mesocyclone activity over the North-East Atlantic. Part 1: vortex distribution and variability. *Int. J. Climatol.* **19**, 1187–1204.

Hoskins, B. J. and Hodges, K. I. 2005. A new perspective on Southern Hemisphere storm tracks. *J. Clim.* **18**, 4108–4129.

Inatsu, M. and Hoskins, B. J. 2004. The zonal asymmetry of the Southern Hemisphere winter storm track. *J. Clim.* **17**, 4882–4892.

Jolliffe, I. T. 2002. *Principle Component Analysis*. Springer-Verlag, New York.

Kalnay, E., Kanamitsu, M., Kistler, R., Collins, W., Deaven, D. and co-authors. 1996. The NCEP/NCAR 40-year reanalysis project. *Bull. Am. Meteorol. Soc.* **77**, 437–471.

Karoly, D. J. 1989. Southern Hemisphere circulation features associated with El Nino-Southern Oscillation events. *J. Clim.* **2**, 1239–1252.

Kolstad, E. W. and Bracegirdle, T. J. 2008. Marine cold-air outbreaks in the future: an assessment of IPCC AR4 model results for the Northern Hemisphere. *Clim. Dyn.* **30**, 871–885.

Kolstad, E. W., Bracegirdle, T. J. and Seierstad, I. A. 2009. Marine cold-air outbreaks in the North Atlantic: temporal distribution and associations with large-scale atmospheric circulation. *Clim. Dyn.* **33**, 187–197, doi:10.1007/s00382-008-0431-5.

Laing, A. K. and Reid, S. J. 1999. Evidence of mesoscale lows off the west coast of New Zealand. *Wea. Forecast.* **14**, 369–383.

Lau, K. M., Sheu, P. J. and Kang, I. S. 1994. Multiscale Low-Frequency Circulation Modes in the Global Atmosphere. *J. Atmos. Sci.* **51**, 1169–1193.

Limpasuvan, V. and Hartmann, D. L. 2000. Wave-maintained annular modes of climate variability. *J. Clim.* **13**, 4414–4429.

Marshall, G. J. 2002. Trends in Antarctic geopotential height and temperature: a comparison between radiosonde and NCEP-NCAR reanalysis data. *J. Clim.* **15**, 659–674.

Marshall, G. J. 2007. Half-century seasonal relationships between the Southern Annular Mode and Antarctic temperatures. *Int. J. Climatol.* **27**, 373–383, doi:10.1002/joc.1407.

Mo, K. C. 2000. Relationships between low-frequency variability in the Southern Hemisphere and sea surface temperature anomalies. *J. Clim.* **13**, 3599–3610.

Økland, H. 1998. Modification of frontal circulations by surface heat flux. *Tellus* **50A**, 211–218.

Rasmussen, E. A. and Turner, J. 2003. *Polar Lows: Mesoscale Weather Systems in the Polar Regions*. Cambridge University Press, Cambridge, UK.

Thompson, D. W. J. and Wallace, J. M. 2000. Annular modes in the extratropical circulation. Part I: month-to-month variability. *J. Clim.* **13**, 1000–1016.

Vavrus, S., Walsh, J. E., Chapman, W. L. and Portis, D. 2006. The Behaviour of extreme cold air outbreaks under greenhouse warming. *Int. J. Climatol.* **26**, 1133–1147.